Supplementary Information (SI) for JAAS.

Supplementary materials to accompany: "Determining the sources of (sub)permil-level inaccuracy during laser ablation-MC-ICPMS boron isotope measurements of carbonates"

Douglas Coenen, David Evans, Hana Jurikova, Matthew Dumont, James Rae, Wolfgang Müller

FTIR characterisation of magnesite and dolomite

The composition of the geological samples of dolomite and magnesite utilised here was confirmed via attenuated total reflectance Fourier transform infrared spectroscopy (ATR-FTIR). Samples were crushed using an agate mortar and measured using a Bruker Platinum ATR infrared spectrometer fitted with a TGS detector at Goethe University Frankfurt. Measurements were performed at 1 cm^{-1} resolution with 32 scans. A baseline measurement was performed before every sample. Figure S1 displays the results of these analyses, focusing on ν_4 CO_3 vibration maxima (in-plane bend), the position of which strongly depends on the samples Mg/Ca.

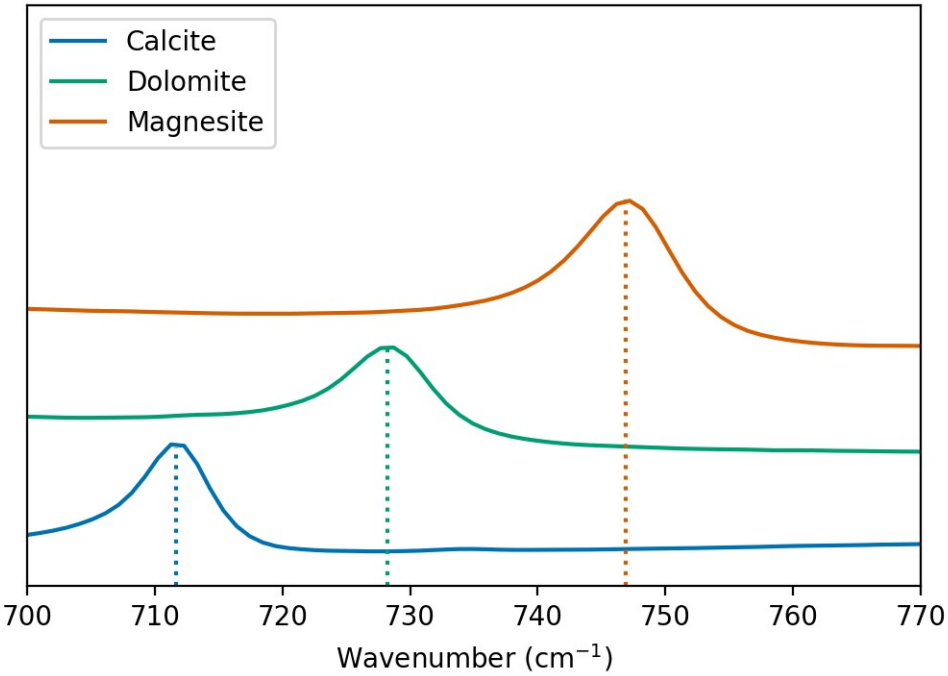

Figure S1: FTIR spectra of powdered calcite, dolomite and magnesite. The y-axis has arbitrary units and the three spectrums are separated by an artificial factor for enhanced readability. The coloured dashed lines are the corresponding literature values for each mineral found in the RRUFF database (Lafuente et al., 2015).

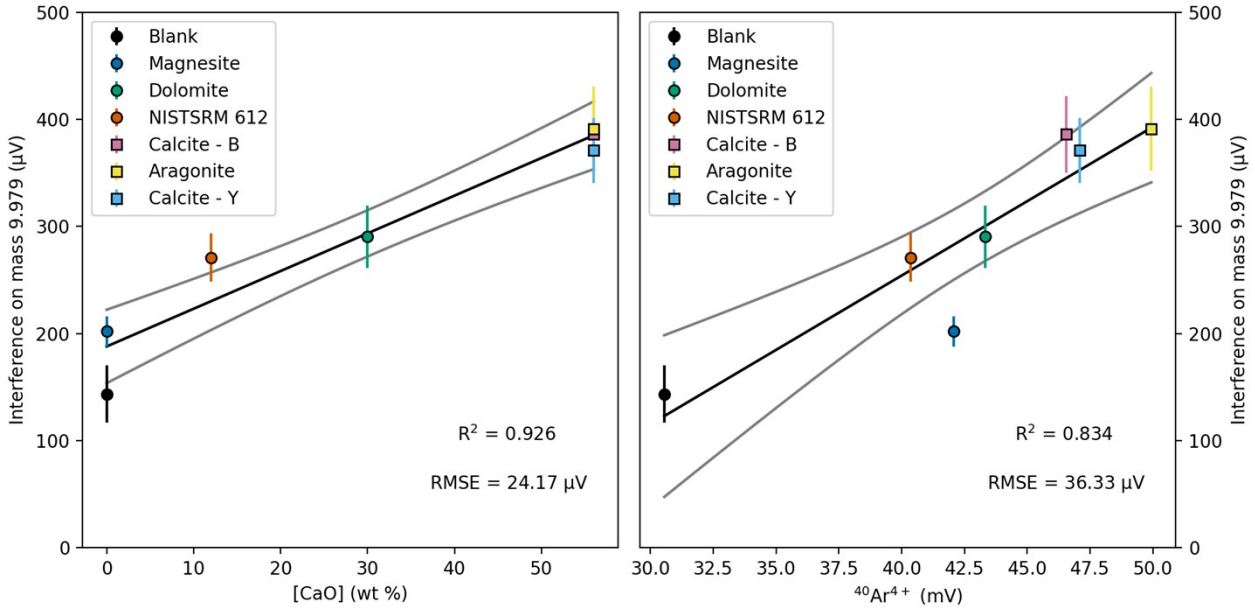

Figure S2: The interference on m/z 9.979 as a function of [CaO] of the analyte matrix (a) and measured $^{40}Ar^{4+}$ ion beam intensity (b).

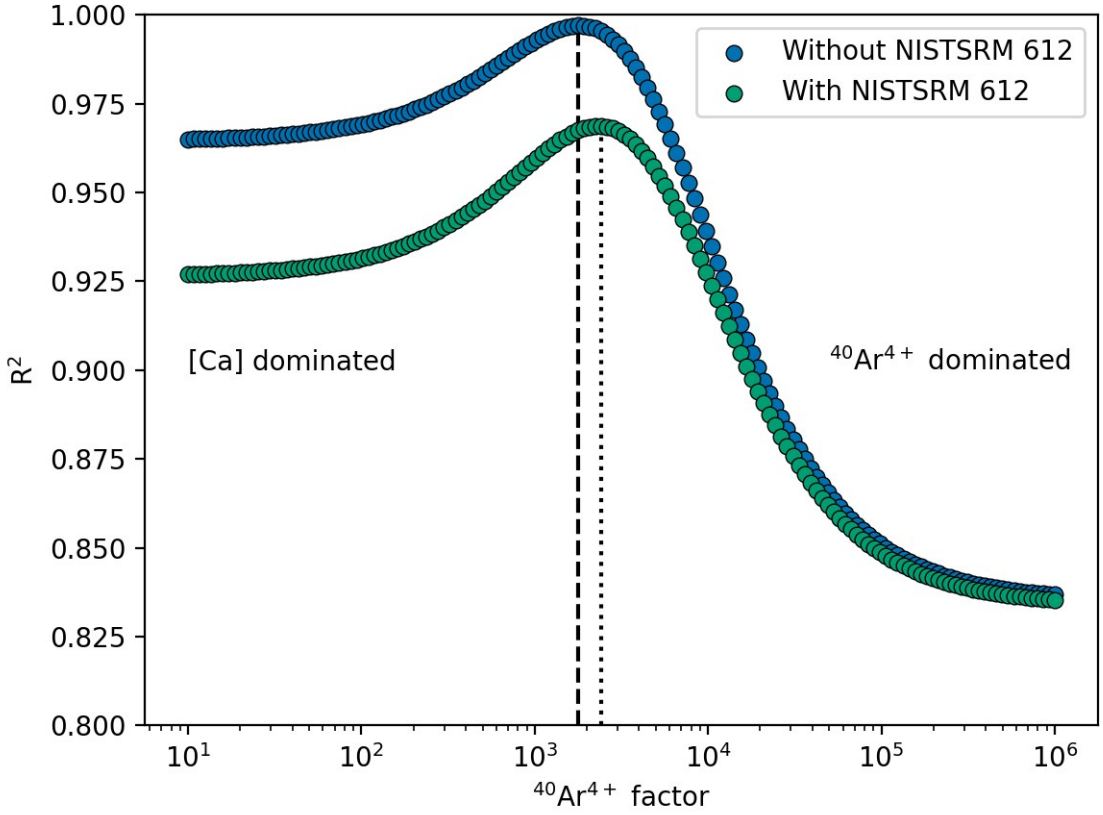

Figure S3: Determination of the impact of our $^{40}Ar^{4+}$ factor on the goodness of fit of the regression between the combined [Ca] plus $^{40}Ar^{4+}$ interference and the baseline elevation centred around m/z ≈ 10. The R^2 value was calculated from a linear regression between the [CaO] of the analyte plus the measured $^{40}Ar^{4+}$ ion beam intensity multiplied by the unitless factor displayed above against the measured background elevation at m/z = 9.979 (see Fig. 3b in the main text). The $^{40}Ar^{4+}$ factor yielding the best fit when performing the linear regression without NISTSRM 612 (displayed in blue) has a value of ~1810 (displayed as the dashed vertical line; used in Figure 3b), while the linear regression including the measurement of NISTSRM 612 (displayed in green), has a unitless $^{40}Ar^{4+}$ factor of ~2310 (displayed by the dotted line; used in Figure S4). Each factor is unique to its dataset and changes with different analytical session and/or instrumental tuning.

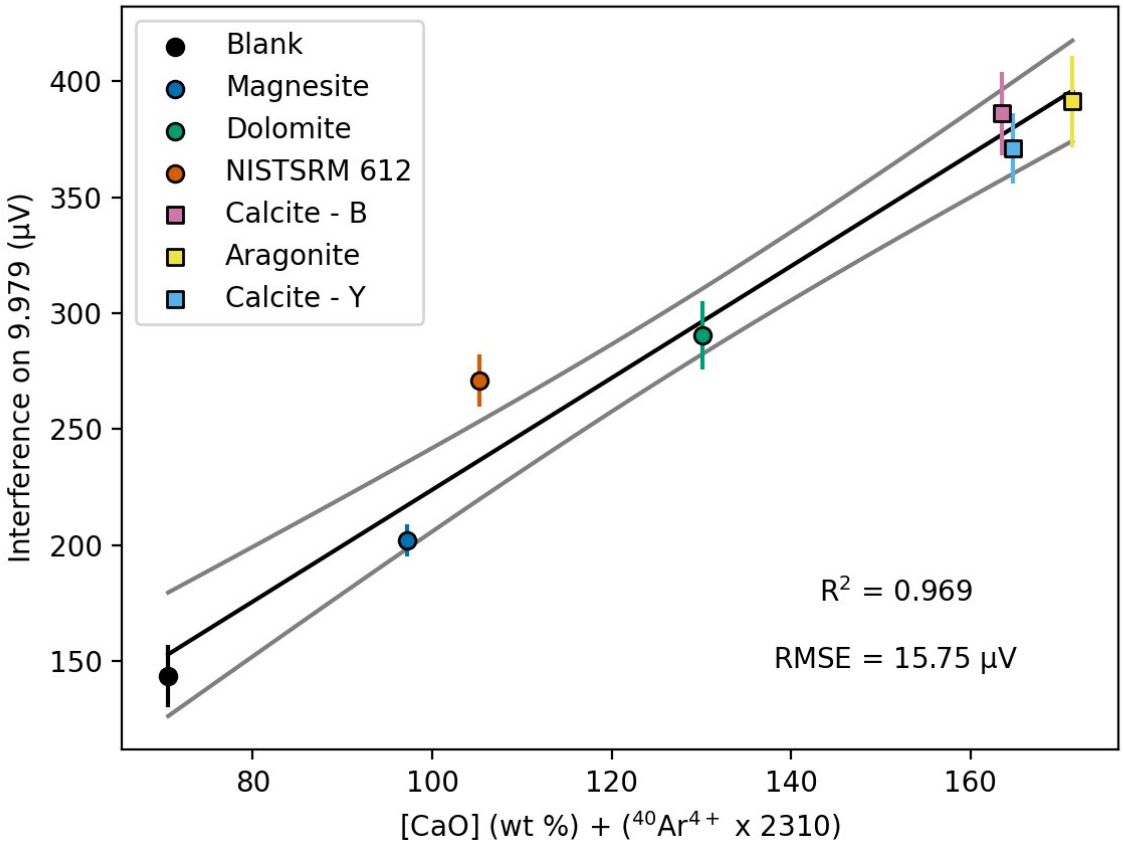

Figure S4: Average background elevation during the ablation of a suite of carbonate samples (including NISTSRM 612) at m/z ≈ 9.979 as a function of matrix [CaO] and $^{40}Ar^{4+}$ ion beam intensity multiplied by a unitless factor (see main text). The displayed uncertainty is the 2 SE of the voltage between m/z ≈ 9.9 and 9.98. The unitless factor was optimised for this dataset by performing the same methodology shown in Figure S3, green dots.

Table S1: Ablation rates of common carbonate materials, many of which are used a standards for boron isotope measurements using LA-MC-ICPMS. This data is displayed in Figure 5 (main text). PP = "pressed pellet", NP = "nano pellet", Ara. = "aragonite", Cal. = "calcite", Gla. = "glass".

Sample	Laser fluence (J/cm^2)	Ablation rate (nm/pulse)	Ablation rate 2 SD (nm/pulse)
JCP-1-PP	6	368.5	59.4
JCt-1-PP	6	384.9	52.4
MACS-3-PP	2	142.8	6.3
	6	348.6	53.6
	10	487.8	27.7
MACS-3-NP	6	293.0	25.0
JCp-1-NP	6	250.0	23.2
JCt-1-NP	6	233.2	39.2
KCSp-NP	2	141.7	7.2
	6	265.5	14.2
	10	346.0	20.2
Tridacna-Ara.	6	184.5	8.0
UWC-1-Cal.	6	189.8	16.1
UWC-3-Cal.	6	188.5	11.3
DE-B-Cal.	2	102.0	9.2
	6	191.6	15.8
	10	255.3	6.8
DE-Y-Cal.	2	99.6	7.4
	6	186.5	14.6
	10	253.2	6.8
NIST SRM 612-Gla.	6	181.9	6.3

References

Lafuente B, Downs R T, Yang H, Stone N (2015) The power of databases: the RRUFF project. In: Highlights in Mineralogical Crystallography, T Armbruster and R M Danisi, eds. Berlin, Germany, W. De Gruyter, pp 1-30